Incorporation of First-Order Uptake Rate Constants from Simple Mammillary Models into Blood-Flow Limited Physiological Pharmacokinetic Models via Extraction Efficiencies

William L. Roth,[1,3] L. W. D. Weber,[1,2] and Karl K. Rozman[1,2]

Received April 19, 1994; accepted September 7, 1994

Incorporation of First-Order Uptake Rate Constants from Simple Mammillary Models into Blood-Flow Limited Physiological Pharmacokinetic Models via Extraction Efficiencies. W. L. Roth, L. W. D. Weber, and K. Rozman (1995). Pharm. Res. 263–269. First-order rate constants obtained from classical pharmacokinetic models correspond to mammillary systems in which all of the blood (or plasma) is assumed to be located in a central compartment. In such models the rate at which chemicals are transported out of this pool and into another compartment is the product of the mass of chemical in the central compartment multiplied by a rate constant, which is not limited in magnitude by the blood flow, or the rate at which chemicals from the blood are delivered to the peripheral compartment. Most of the physiologically-based models published to date dispense with some of the information available from mammillary models by assuming that all of the chemical delivered by the flow of blood rapidly equilibrates and can be taken up by the tissue under the control of a "partition coefficient" ($R_{ij} = C_j/C_i$). We show that the partition coefficient alone does not retain the uptake rate (k_{ji}) information available from a classical mammillary model, but that the uptake rate information can be incorporated via unitless extraction efficiency parameters, ϵ_j.

KEY WORDS: tissue uptake; extraction efficiency; blood flow-limited models; 2,3,7,8-tetrachlorodibenzo-p-dioxin.

INTRODUCTION

From the late 1950's through the late 1970's, the majority of pharmacokinetic models described in the literature were variations of 2, 3 or more compartments with a central pool representing blood, plus surrounding compartments representing tissues, grouped into "slow" and "fast" compartments (1). Over the last decade, the use of blood-flow limited, or "physiologically-based" pharmacokinetic models has become widespread, generally incorporating five or more compartments (2). These models are usually constructed around a set of measured (or agreed upon) blood flows to specific tissues, which may be lumped into groups described as "richly perfused" and "poorly perfused", in the same manner as the mammillary models would contain "fast" and "slow" compartments. "Physiologically-based" models may also contain reaction rate constants describing metabolism, and specific binding coefficients for chemicals that are known to bind to specific proteins or receptors. However, transport between blood and tissues has usually been described only in terms of blood flows and partition coefficients under the assumption that blood flow, rather than permeability is limiting. For many chemicals this assumption is invalid, and has required modelers to replace blood flow terms with alternative parameters which reduce the effective mass of chemical delivered to the tissue by the blood.

Examples of such equivalent formulations are found in Farris et al. (3), where blood flows (Q_js) were replaced by "intercompartmental transport parameters" (k_js), and Kedderis et al. (4), in which Q_js were replaced with "diffusive clearances" or "permeability-surface area products" $PA_j = fQ_j$. Here "f" is a unitless fraction which was unnamed (4), but which is equivalent to the "extraction" (E(t)) used by other authors (5–7) in modeling the transport of metal ions and nutrients in the physiological literature. We have employed a limiting case of the extraction, E(t), evaluated between the time of entry of a bolus of a tracer into the arterial side of a tissue's vasculature and the time (τ) required for the unextracted fraction ($1 - E(\tau)$) to reach outflow on the venous side. We call the limiting value of E(t) an extraction efficiency, ϵ, and show with examples for a variety of tissues that the uptake rate information available from classical mammillary models can be incorporated into blood flow-limited models by computing the corresponding extraction efficiency using each tissue-specific blood flow and mammillary model uptake rate.

THEORY

Figure 1a is an example of a three compartment mammillary model, with first-order transport rate constants for tissue uptake (k_{21}, k_{31}), recycling (k_{12}, k_{13}) and elimination (k_{02}) as the only model parameters. The equations describing this system are

$$\frac{dM_1}{dt} = U(t) + k_{12}M_2 + k_{13}M_3 - (k_{21} + k_{31})M_1 \quad (1)$$

$$\frac{dM_2}{dt} = k_{21}M_1 - (k_{12} + k_{02})M_2 \quad (2)$$

$$\frac{dM_3}{dt} = k_{31}M_1 - k_{13}M_3 \quad (3)$$

In this case M_1 represents the mass of a chemical in the blood, M_2 its mass in the liver, and M_3 the balance of the dose in muscle or carcass. U(t) is an arbitrary input function. Each of the rate constants is an idealized first-order parameter, having units of reciprocal time. The most commonly used representation of such a system in a "physiologically-based" (blood flow-limited) pharmacokinetic model is (Figure 1b)

[1] Department of Pharmacology, Toxicology, and Therapeutics, University of Kansas Medical Center, 3901 Rainbow Blvd., Kansas City, Kansas 66160.

[2] Section of Environmental Toxicology, GSF-Institut für Toxikologie, 85758 Neuherberg, Germany.

[3] Present address: U.S. FDA, MOD-1 Laboratory, 8301 Muirkirk Rd., Laurel, Maryland 20708

0724-8741/95/0200-0263$07.50/0

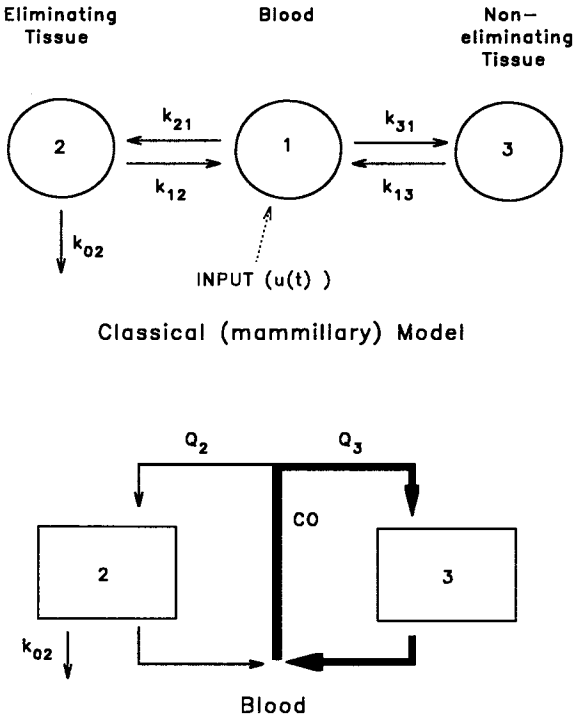

Figure 1 a) Example of a three compartment mammillary model with first order transport rate constants: tissue uptake (k_{21}, k_{31}), recycling (k_{12}, k_{13}) and elimination (k_{02}). (b) Physiologically-based equivalent model for the mammillary model in (a). The corresponding equations are 4–6. Note that ϵ_js would accompany Q_js in this diagram.

$$\frac{dM_1}{dt} = U(t) - Q_2(C_1 - C_2/R_{12}) - Q_3(C_1 - C_3/R_{13}) \quad (4)$$

$$\frac{dM_2}{dt} = Q_2(C_1 - C_2/R_{12}) - k_{02}C_2V_2 \quad (5)$$

$$\frac{dM_3}{dt} = Q_3(C_1 - C_3/R_{13}) \quad (6)$$

where

Q_j = blood flow to compartment j
C_j = concentration of substance in compartment j
R_{ij} = tissue-to-blood partition coefficient
V_j = volume of compartment j

If we set the mammillary and physiologically-based model equations for M_3 equal, and substitute concentration and volume terms for M_3, we obtain

$$k_{31}M_1 - k_{13}M_3 = k_{31}C_1V_1 - k_{13}C_3V_3 = Q_3C_1 - Q_3C_3/R_{13}$$

If all compartments start at $C_j = 0$, and an input U(0) is placed in compartment 1, then $C_3 = 0$ at $t = 0$, and $k_{31}C_1V_1 = Q_3C_1$. In the reciprocal case, the input U(t) is placed in compartment 3, $C_1 = 0$ at $t = 0$, and $k_{13}C_3V_3 = Q_3C_3/R_{13}$. Provided that this model is an accurate representation of transport between blood and tissue, it follows that $k_{31} = Q_3/V_1$ and $k_{13} = Q_3/V_3R_{13}$. This implies that the first-order uptake rate (k_{31}) is equal to the fraction of the total blood volume (V_1) that passes through tissue j, ie. that 100% of the chemical passing through the tissue is extracted during the first pass, when the tissue concentration is near zero. Since substantial barriers to free exchange are known to exist between blood and tissues, this assumption will clearly be unsuitable for many, if not most chemicals. In studying the uptake of a chemical brought to a tissue by the arterial flow Crone (5) defined the extraction E(t) as

$$E(t) = [h_N(t) - h_D(t)]/h_N(t) \quad (7)$$

where

h_N is the fraction of an injected nonextractable substance recovered at the venous outflow at time t,

h_D is the fraction of an injected extractable substance recovered at the venous outflow at time t.

Since the fraction of "D" entering at the arterial side = 1.0, this is the same as writing

$$E(\tau) = [h_{art}(0) - h_{venous}(\tau)]/h_{art}(0) \quad (8)$$

In order to describe the extraction of a tracer that may be introduced at a time τ relative to time t, we define

$$\epsilon = \lim_{t \to \tau} [E(t)] \quad (9)$$

We have incorporated this simple, unitless extraction efficiency, ϵ_j, into our physiologically-based models as a means of representing the barrier to uptake. *This parameter represents the fraction of a mass of chemical delivered to a tissue j, at an arterial concentration C_j and blood flow Q_j, that can cross from the blood to the tissue side of the barrier during the time τ required for a single transit of the tissue.*

With the addition of ϵ_js, physiological model equations (4) through (6) are written

$$\frac{dM_1}{dt} = U(t) - \epsilon_2Q_2(C_1 - C_2/R_{12}) - \epsilon_3Q_3(C_1 - C_3/R_{13}) \quad (10)$$

$$\frac{dM_2}{dt} = \epsilon_2Q_2(C_1 - C_2/R_{12}) - k_{02}C_2V_2 \quad (11)$$

$$\frac{dM_3}{dt} = \epsilon_3Q_3(C_1 - C_3/R_{13}) \quad (12)$$

The effect of incorporating ϵ_js on tissue uptake curves is illustrated in Figure 2 using the equivalent physiological pharmacokinetic model (Figure 1a). Note that the principal effect is a reduction of the maximum concentration of a chemical achieved in the eliminating tissue, in addition to shifting the peak concentration to the right along the time axis. It should also be noted that reducing ϵ lengthens the time required to reach steady-state, since the barrier presented by ϵ_j in this formulation affects the rate of transport bidirectionally. Useful relationships between mammillary model rate constants and physiological model parameters can then be derived:

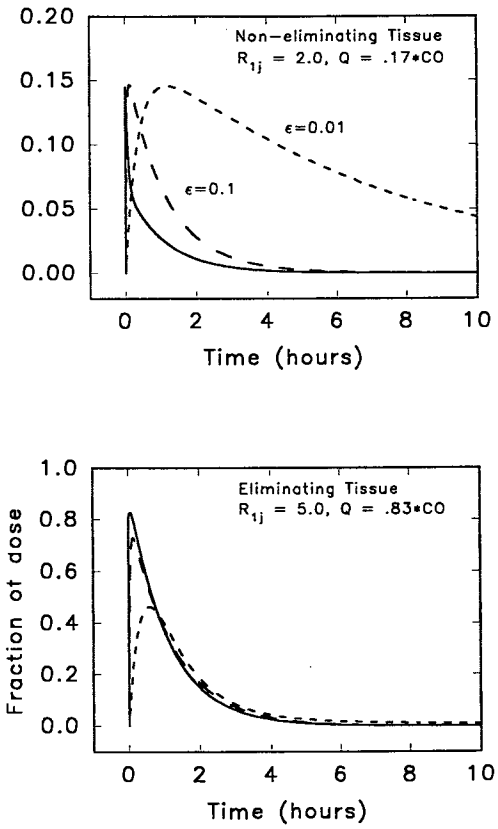

Figure 2 Predicted fractions of dose in peripheral compartments of the model in Figure 1b when ϵ_js are incorporated into the model equations. The solid lines represent model behavior when $\epsilon = 1$. The principal effects of decreasing this parameter are to shift the tissue concentration peak and reduce the concentration in eliminating tissues.

$$k_{31}C_1V_1 - k_{13}C_3V_3 = \epsilon_3Q_3(C_1 - C_3/R_{13}) \quad (13)$$

When concentration terms are equated:

$$(k_{31}V_1 - \epsilon_3Q_3)C_1 = (k_{13}V_3 - \epsilon_3Q_3/R_{13})C_3 \quad (14)$$

At $t = 0$, $C_3 = 0$, implying that $k_{31}V_1 = \epsilon_3Q_3$, and $\epsilon_3 = k_{31}V_1/Q_3$. Setting $C_2 = 0$ at $t = 0$ in equation (11) results in an analogous expression of the generalized form

$$\epsilon_j = \frac{k_{j1}V_1}{Q_j} \quad (15)$$

It should be noted that other parameters such as the tissue permeability (P), and active transport rate constants can be obtained once the extraction has been characterized, if other information such as the total capillary surface area (S) and the relationship between plasma concentration and uptake rate are known (8). The incorporation of ϵ terms does not affect the meaning or computation of the partition coefficients, R_{1j}. If R_{1j} is the concentration ratio C_j/C_1 at steady-state, and there is no elimination from compartment j, rearrangement of the terms of the mammillary model gives

$$\frac{dM_jss}{dt} = 0 \quad ; k_{ji}C_1ssV_1 = k_{1j}C_jssV_j \quad (16)$$

$$R_{1j} = \frac{k_{j1}V_1}{k_{1j}V_j} = \frac{C_jss}{C_1ss} \quad (17)$$

When first-order elimination occurs from j, k_{0j} must be added to the denominator

$$k_{j1}C_1ssV_1 = (k_{1j} + k_{0j})C_jssV_j \quad (18)$$

and

$$R_{1j} = \frac{k_{j1}V_1}{(k_{1j} + k_{0j})V_j} \quad (19)$$

The relationships derived above were used to estimate extraction efficiencies and partition coefficients for a variety of tissues in rats treated with the toxic compound 2,3,7,8-tetrachlorodibenzo-p-dioxin (TCDD) as described in the next section.

DATA AND METHODS

The set of data described in the "Results" section was taken from tables of tissue concentrations contained in reference 9. Values for first-order uptake and tissue-to-blood recycling rates were estimated by assuming that each tissue was the second compartment of a two compartment model, in which the first compartment, the blood, had been fitted with a 3-exponential model:

$$M_1(t) = A_0e^{-k1t} + B_0e^{-k2t} + C_0e^{-k3t} \quad (20)$$

The tissue equation

$$\frac{dM_j}{dt} = k_{j1}M_1 - (k_{1j} + k_{0j})M_2 \quad (21)$$

was solved algebraically be substituting the 3-exponential equation for M_1, giving

$$M_j(t) = k_{j1}\left\{\frac{A_0(e^{-Ejt} - e^{-k1t})}{k_1 - E_j} + \frac{B_0(e^{-Ejt} - e^{-k2t})}{k_2 - E_j} + \frac{C_0(e^{-Ejt} - e^{-k3t})}{k_3 - E_j}\right\} + M_j(0)e^{-Ejt} \quad (22)$$

The resulting equation was coded into curve fitting algorithms in the SigmaPlot (Ver. 4.1) program, along with initial estimates of uptake and elimination rates. Initial optimization efforts utilized the Marquadt-Levenberg scheme. Further improvements were obtained through iteration of equivalent algorithms encoded in SAAM (10) and/or manual iteration via the SigmaPlot Math Transform solver.

RESULTS

As shown in Figure 3, a very good 3-exponential fit was obtained for the blood during the first week of the experimental observations. The model diverges from the observed data after this time, as a result of pharmacodynamic changes in the animals (associated with TCDD toxicity) that are the subject of other papers (11,12). The fitted parameters for the blood were incorporated into the two-compartment curve fitting equations to obtain parameters for other tissues.

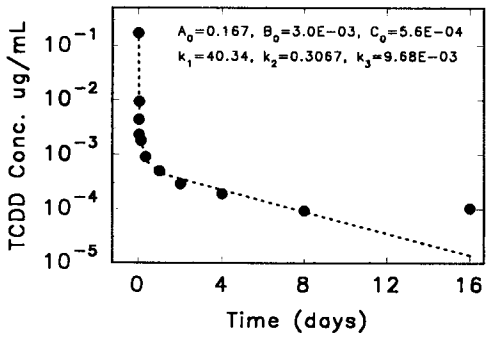

Figure 3 Three exponential model fit to concentration data for TCDD in blood after an intravenous dose of 9.25 ug/kg. The rise in concentration after 12 days is a pharmacodynamic effect resulting from body weight loss.

Parameter estimation results for the tissues studied can be divided into two classes: a) those consisting of only one kinetically identifiable compartment (lung and muscle; Figure 4), and (b) those containing a fat-like component that results in two (or more) kinetically identifiable compartments (white adipose tissue [WAT], brown adipose tissue [BAT], and kidney; Figure 5). In the latter cases one set of parameters was derived to fit the rapid uptake and depuration portion of the curve, while a fat-like set of parameters was scaled to the "slow" portion of the curve so that the sum of the two components resembled the overall behavior of the curve.

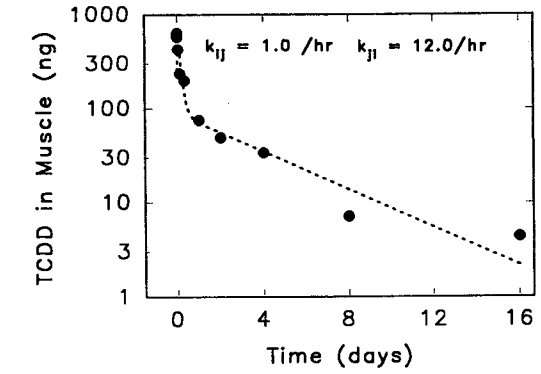

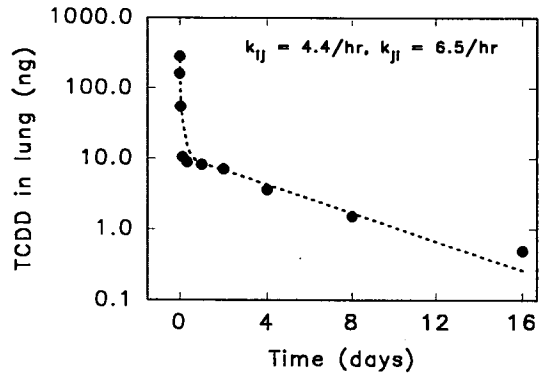

Figure 4 Data and simulations using best-fitting parameters for Equation 22 in tissues with only one kinetically significant compartment. Some pharmacodynamic effects associated with weight loss are evident at later time points.

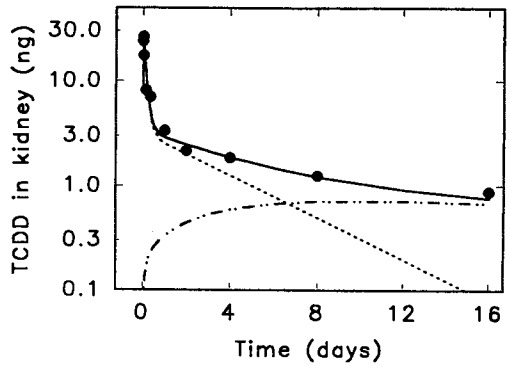

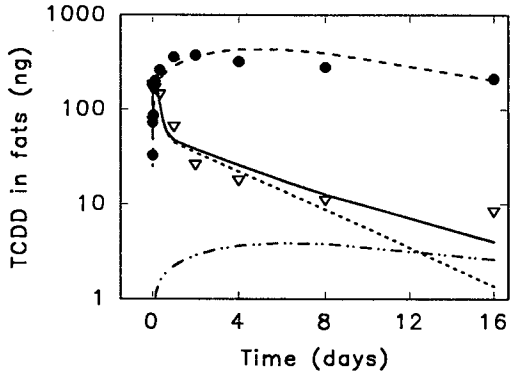

Figure 5 Data and simulations using best-fitting parameters for Equation 22 in tissues containing two or more kinetically observable compartments. TCDD concentrations in fats are plotted as one graph: solid circles (●) represent TCDD in WAT, open triangles (▽) TCDD in BAT. In each case the solid line (——) represents the sum of two compartments, which are plotted as dotted (Phase 1) or dashed lines (Phase 2) in the same figures. Parameter values for the fitted curves are listed in Table II.

Table I lists blood flows and tissue volumes used in the computation of extraction efficiencies and partition coefficients that are summarized in Table II. Table II lists estimated uptake rate constants (k_{j1}), recycling rate constants, (k_{1j}), extraction efficiencies, (ϵ_j), and tissue/blood partition coefficients (R_{1j}) for tissues in category "a" and "b". Note that the ϵ_js allow uptake of less than 10 % ($\epsilon_j < 0.10$) of the mass of chemical delivered to the tissue in all type "a" tissues. Extraction efficiencies for WAT and BAT were higher, exceeding 10 % of the delivered mass. In other type "b" tissues the values of ϵ_j and R_{1j} were less certain because of the complex nature of the compartment kinetics. The thymus and kidney had very low extraction efficiencies for TCDD ($\epsilon_j < 0.01$), but nevertheless exhibited 2 compartment behavior that we assume represents small lipid compartments within these tissues. Rather different trends were observed when the ϵ_js were expressed on a per gram basis. Skin and muscle had the lowest extraction, while the spleen and kidney, which had low total extraction efficiencies, had high efficiencies when expressed on a per gram basis.

In Figure 6, a comparison is made between predictions of WAT and liver concentrations of TCDD using a model (12)

Table I. Organ Blood Flows[a] (Q_j), Weights (V_j) and Blood Volumes of Male Rats at 240 g Body Weight

Organ	Fractional flow[b] (fCO)	Weight (g)	V_j/Q_j	Organ[e] blood (μL)
White Fat (WAT)	0.022	15.85	9.420	—
Brown Fat (BAT)	0.028	3.00	1.570	—
Muscle	0.400	140.8	4.570	2379
Kidney	0.160	2.08	0.163	414
Small Intestine	0.104	3.72	0.467	63
Large Intestine	0.027	3.09	1.495	202
Spleen	0.017	0.635	0.488	267
Skin	0.110	24.85	2.972	315
Brain	0.020	1.91	1.240	42
Lung	1.00[c]	1.375	0.018	1268
Liver	0.210[d]	11.22	0.703	3398

[a] Values taken from references 11 and 12.
[b] fCO = fraction of cardiac output. CO for a male rat at 240 grams of body weight is approximately 4588 mL/hr = 76 mL/min = 1.27 mL/sec. This translates into about six complete circulations of the total blood volume per minute.
[c] It is assumed here that the total CO perfuses the lung.
[d] Includes hepatic artery, which accounts for 0.05 * CO.
[e] Calculated from reference 22.

operated under three related scenarios: (a) with best-fit partition coefficients R_{1j} and all ϵ_js set to 1.0 (flow-limiting case), (b) the same partition coefficients plus ϵ_js from Table II, and (c) the same model with ϵ_js and R_{1j}s optimized from the initial estimates obtained by the methods described here, as listed in Table II. Note the improvement in fit, especially during the uptake phase of the curves. Plots have been made on both linear and log scales. Log scales tend to hide errors in fit of the uptake phase of less than 200%, while linear plots hide errors in fit of the elimination phase.

DISCUSSION

The permeability and passage of chemicals through capillary walls into tissues was first reviewed by Pappenheimer (13). The concept of extraction, which includes not only the permeability of membranes to a chemical, but also its interactions with blood or plasma carriers, has been theoretically treated by several authors (7,14), and has been used to describe the transport of a variety of substances including alkali metal ions (6,15), galactose (8), urea (16), dyes (17), fatty acids (11,18,19), anesthetics (20), and therapeutic antibody-drug combinations (21). The majority of "physiologically-based" models that have been published do not incorporate information or set limits on the rate of uptake of chemicals by tissues, beyond the limitation imposed by fixed blood flows. Many of these models were developed to predict the distribution of volatile solvents, which diffuse through lipophilic membranes very rapidly, and reach states of equilibrium fast enough to be described with considerable accuracy by partition coefficients alone. However, many chemicals do not diffuse rapidly enough to reach a partitioning equilibrium between tissues and blood, and require better description of transport limitations to be modeled.

The approach described here has several limitations. It first should be emphasized that in applying a single parameter to represent the permeability barrier at the cell membrane, we are assuming that there is parity to this barrier such that it is the same whether entering or leaving the compartment. While this gives us more information with which to describe transport between compartments than a simple partition coefficient, such barriers are unlikely to be the same in both directions for many chemicals. Where the use of a single ϵ is insufficient, reformulation of the mass balance equations would allow the use of individual permeabilities for uptake and recycling. In computing uptake rate constants with the deconvolution technique described in Methods, no

Table II. Estimated Tissue-Blood Transport Parameters for 2,3,7,8-Tetrachlorodibenzo-p-dioxin (TCDD)

Tissue	Uptake k_{j1} (1/hr)	Recycling k_{1j} (1/hr)	Extraction efficiency ϵ_j	Extraction efficiency ϵ_j/g ($\times 10^3$)	Partition coefficient R_{1j}
Brain	0.05	0.35	0.0071	3.72	0.97
Lung	6.50	4.40	0.0198	14.40	13.9
Muscle	12.0	1.00	0.0989	0.71	1.31
Liver[a]	—	—	0.0350	3.12	9.00
Spleen	0.12	0.55	0.0199	31.34	4.45
Sm. Intestine	0.085	0.085	0.0023	0.62	3.49
Lg. Intestine	0.125	0.105	0.0130	4.21	5.00
BAT	2.30	0.30	0.2599	86.60	33.1
WAT	1.40	0.005	0.1798	11.34	229.0
Kidney	0.50	0.001	0.0088	38.46	2.49 (Phase 1) 6.48 (Phase 2)
Skin	0.63	0.070	0.0162	0.65	4.66 (Phase 1) 20.7 (Phase 2)
Thymus	0.055	0.90	—[b]	—	1.18 (Phase 1) 16.3 (Phase 2)

[a] Since blood flow to the liver is primarily from the portal vein, initial estimates were obtained by computation of the fractional uptake during the distribution phase (ϵ) and linear regression of liver vs blood data in the elimination phase (R_{1j}).
[b] Fractional blood flows for the thymus have not been reported in the literature.

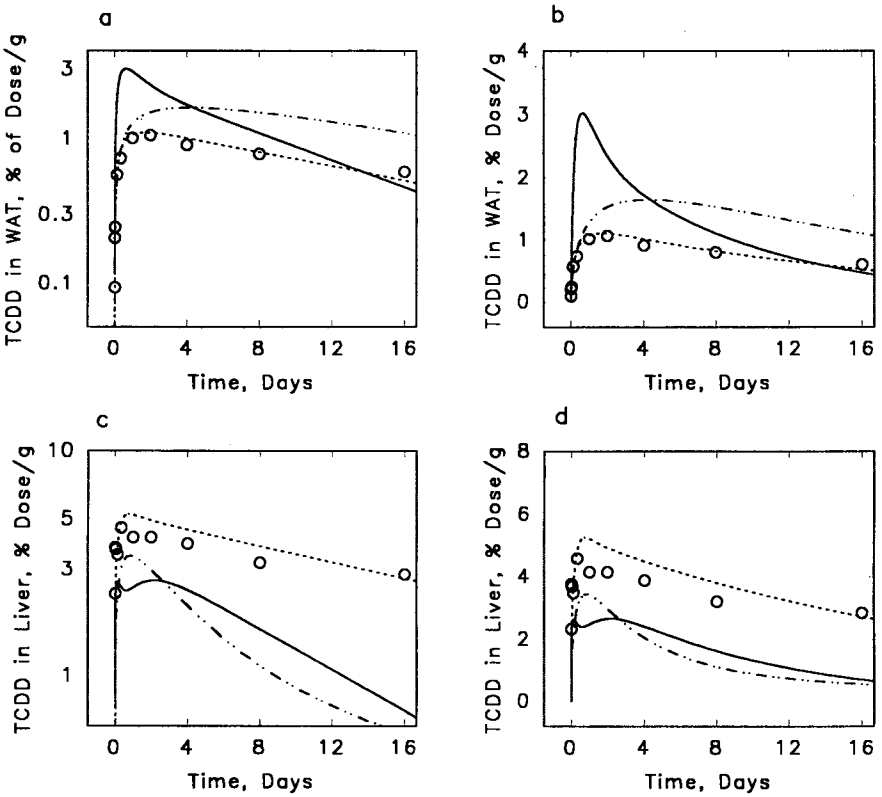

Figure 6 Logarithmic and linear plots of predicted and observed (○) concentrations of TCDD in WAT (a & b) and liver (c & d) generated using three different sets of parameters: solid lines (——) denote concentrations predicted with the partition coefficients of Table II and all ϵ_j set = 1.0, dash-dot (-·-·) with the same partition coefficients with ϵ_j as in Table II, and finally, using optimized parameters (---) as listed in Table I of reference 12. All simulations were performed using the model described in reference 12.

interaction occurs between the blood concentration function and the tissue uptake rate. Consequently the ϵ computed must be optimized in the complete model, which will contain multiple ϵ_j dependencies. It is also impossible to use the average blood concentrations to represent the portal blood concentrations entering the liver. Alternative estimation methods must be used to compute an initial ϵ for the liver. Despite these shortcomings, even this limited information has not been incorporated into the majority of "physiologically-based" models. As a consequence, information on the rate of uptake, which would normally be available via the process of fitting classical 2- and 3- exponential equations to tissue and plasma data, is not represented in most physiological models. Inclusion of ϵ into physiologically-based models allows the inclusion of information on permeability limitations, and should allow the adaptation of simple equilibrium partitioning models to a wider range of substances.

REFERENCES

1) M. Gibaldi and D. Perrier. *Pharmacokinetics,* 2nd edition, Marcel Dekker, New York, 1982.
2) L.E. Gerlowski and R.K. Jain. Physiologically based pharmacokinetic modeling: principles and applications. J. Pharm. Sci. 72(10):1103–1127 (1983).
3) F.F. Ferris, R.L. Dedrick, P.V. Allen, J.C. Smith. Physiological model for the pharmacokinetics of methyl mercury in the growing rat. Toxicol. Appl. Pharmacol. 119(1):74–90 (1993).
4) L.B. Kedderis, J.J. Mills, M.E. Andersen, L.S. Birnbaum. A physiologically based model for 2,3,7,8-tetrabromodibenzo-p-dioxin (TBDD) in the rat: tissue distribution and CYP1A induction. Toxicol. Appl. Pharmacol. 121:87–98 (1993).
5) C. Crone. Permeability of capillaries in various organs as determined by the use of the "indicator diffusion" method. Acta Physiol. Scand. 58:292–305 (1963).
6) E.M. Renkin. Transport of potassium-42 from blood to tissue in isolated mammalian skeletal muscles. Am. J. Physiol. 197(6): 1205–1210 (1959).
7) C.A. Goresky, W.H. Ziegler, G.G. Bach. Capillary exchange modeling: barrier-limited and flow-limited distribution. Circ. Res. 27:739–764 (1970).
8) C.A. Goresky, G.G. Bach, B.E. Nadeau. On the uptake of materials by the intact liver. The transport and net removal of galactose. J. Clin. Invest. 52:991–1009 (1973).
9) L.W.D. Weber, S.W. Ernst, B.U. Stahl, K. Rozman. Tissue distribution and toxicokinetics of 2,3,7,8-tetrachlorodibenzo-p-dioxin in rats after intravenous injection. Fund. Appl. Toxicol. 21(4):523–534 (1993).
10) R.C. Boston, P.C. Greif, M. Berman. Conversational SAAM—an interactive program for kinetic analysis of biological systems. Computer Prog. Biomed. 13:111–119 (1981).
11) W.L. Roth, L.W.D. Weber, B.U. Stahl, K. Rozman. A pharmacodynamic model of triglyceride transport and deposition during feed deprivation or following treatment with 2,3,7,8-tetrachlorodibenzo-p-dioxin (TCDD) in the rat. Toxicol. Appl. Pharmacol. 120:126–137 (1993).
12) W.L. Roth, S. Ernst, L.W.D. Weber, L. Kerecsen, K. Rozman. A pharmacodynamically responsive model of 2,3,7,8-tetrachlorodibenzo-p-dioxin (TCDD) transfer between liver and fat

at low and high doses. Toxicol. Appl. Pharmacol. 127:151–162 (1994).
13) J.R. Pappenheimer. Passage of molecules through capillary walls. J. Clin. Invest. 33:387–423 (1953).
14) J.B. Bassingthwaighte. A concurrent flow model for extraction during transcapillary passage. Circulation Research 35:483–503 (1974).
15) C.A. Goresky, G.G. Bach, B.E. Nadeau. On the uptake of materials by the intact liver. The concentrative transport of rubidium-86. J. Clin. Invest. 52:975–990 (1973).
16) D.J. Bowsher, M.J. Avram, M.C. Frederiksen, A. Asada, A.J. Atkinson. Urea distribution kinetics analyzed by simultaneous injection of urea and inulin: demonstration that transcapillary exchange is rate limiting. J. Pharmacol. Exp. Ther. 230(2):269–274 (1984).
17) E.L. Forker, B.A. Luxon. Albumin-mediated transport of rose bengal by perfused rat liver. J. Clin. Invest. 72:1764–1771 (1983).
18) J. Dancis, V. Jansen, J. Kayden, L. Bjornson, M. Levitz. Transfer across human placenta. III. Effect of chain length on transfer of free fatty acids. Pediat. Res. 8:796–799 (1974).
19) L.A. Hillyard, C.E. Cornelius, I.L. Chaikoff. Removal by the isolated rat liver of palmitate-1-C^{14} bound to albumin and of palmitate-1-C^{14} and cholesterol-4-C^{14} in chylomicrons from perfusion fluid. J. Biol. Chem. 234(9):2240-2245 (1959).
20) S. Bjorkman, J. Akson, F. Nilsson, K. Messeter, B. Roth. Ketamine and midazolam decrease cerebral blood flow and consequently their own rate of transport to the brain: an application of mass balance pharmacokinetics with a changing regional blood flow. J. Pharmacokin. Biopharm. 20(6):637–652 (1992).
21) C. Sung, R.J. Youle, R.L. Dedrick. Pharmacokinetic analysis of immunotoxin uptake in solid tumors: role of plasma kinetics, capillary permeability, and binding. Cancer Research 50:7382–7392 (1991).
22) R.J. Dellenback and G.H. Mulheim. Red blood cell volume and distribution before and after bleed-out in the rat. Am J. Physiol. 198(6):1177–1180 (1960).